

## Orientation statistics of small particles in turbulence

This article has been downloaded from IOPscience. Please scroll down to see the full text article.

2011 New J. Phys. 13 093030

(<http://iopscience.iop.org/1367-2630/13/9/093030>)

View [the table of contents for this issue](#), or go to the [journal homepage](#) for more

Download details:

IP Address: 84.13.225.168

The article was downloaded on 21/09/2011 at 11:00

Please note that [terms and conditions apply](#).

## Orientation statistics of small particles in turbulence

Alain Pumir<sup>1,3</sup> and Michael Wilkinson<sup>2,3</sup>

<sup>1</sup> Laboratoire de Physique, Ecole Normale Supérieure de Lyon, F-69007, Lyon, France

<sup>2</sup> Department of Mathematics and Statistics, The Open University, Walton Hall, Milton Keynes MK7 6AA, UK

E-mail: [alain.pumir@ens-lyon.fr](mailto:alain.pumir@ens-lyon.fr) and [m.wilkinson@open.ac.uk](mailto:m.wilkinson@open.ac.uk)

*New Journal of Physics* **13** (2011) 093030 (18pp)

Received 17 August 2011

Published 20 September 2011

Online at <http://www.njp.org/>

doi:10.1088/1367-2630/13/9/093030

**Abstract.** The statistics of the alignment of axisymmetric microscopic particles in fully developed turbulent flow is studied numerically and theoretically. Direct numerical simulations (DNS) of turbulent flows demonstrate that rod-like particles are more strongly aligned with the vorticity vector than with the principal strain axis. To elucidate this property, we compare the evolution obtained in a turbulent flow with a simpler model, where the velocity gradient of the flow is replaced by a fluctuating random matrix, whose temporal correlations reproduce the properties observed in DNS. In contrast with the DNS results, this model exhibits a strong alignment of the rods with the direction of the fastest stretching of the symmetric part of the random matrix. We argue that the correlation between the rod axis and the vorticity vector arises from similarities between the equations of motion governing these quantities.

<sup>3</sup> Authors to whom any correspondence should be addressed.

**Contents**

<b>1. Introduction</b>	<b>2</b>
<b>2. Orientation statistics in turbulence</b>	<b>4</b>
2.1. Equations of motion . . . . .	4
2.2. Numerical methods . . . . .	4
2.3. Single-time statistics . . . . .	5
2.4. Correlation functions . . . . .	7
<b>3. Stochastic model for velocity gradients</b>	<b>8</b>
3.1. Lagrangian statistics of the velocity gradient . . . . .	8
3.2. A model for the velocity gradient . . . . .	10
3.3. Alignment statistics of the random matrix model . . . . .	11
<b>4. Discussion of the alignment of rods with vorticity</b>	<b>13</b>
4.1. Relation between Jeffery's equation and the vorticity equation . . . . .	13
4.2. Alignment of direction in a random gradient field . . . . .	14
<b>5. Concluding remarks</b>	<b>16</b>
<b>Acknowledgments</b>	<b>17</b>
<b>References</b>	<b>17</b>

**1. Introduction**

The motion of microscopic axisymmetric objects in a fluid flow was first considered by Jeffery [1], who determined the equation of motion for the direction of the axial vector  $\mathbf{n}$ . The rotation of this vector is determined by the Lagrangian velocity gradient tensor  $\mathbf{A}(t)$ , defined by  $A_{ij} = \partial u_i / \partial x_j$ , where  $\mathbf{u}(\mathbf{r}, t)$  is the velocity of the fluid. Jeffery [1] applied his equation to analyse the viscosity of a suspension of rods in a simple shear flow, and this work formed a basis for the study of the rheology of liquid crystals (see, e.g., [2, 3]). In some contexts it is of interest to understand the textures of the direction vector field  $\mathbf{n}(\mathbf{r}, t)$  formed by a suspension of microscopic particles in a complex flow [4, 5] and the singularities of its order parameter [6, 7]. In this paper, by contrast, we study the temporal evolution of  $\mathbf{n}(t)$  for a single microscopic particle by considering statistics such as the correlation function  $\langle \mathbf{n}(t) \cdot \mathbf{n}(t') \rangle$  (throughout this paper,  $\langle X \rangle$  is the expectation value of  $X$ ). Experimental techniques for measuring such statistics are now becoming available [8–10].

One motivation for considering this problem is that following the orientation of microscopic objects can give experimental information about the velocity gradients in turbulent fluid flows, which is not readily accessible by other approaches. This may be particularly significant for understanding the influence of polymers on fluid flows, because the elongation of polymers is influenced by the velocity gradient of the flow. The studies of fully developed Navier–Stokes turbulence in this paper will be a benchmark against which the orientation statistics in more complex flows can be compared.

Our investigation of microscopic rod-like particles is complementary to those of Shin and Koch [11], who investigated the motion of fibres, which, although small, were longer than the Kolmogorov length of the turbulence. The present work focuses on very small rods and systematically characterizes the alignment between the rods and the velocity gradient tensor.

Our study led to several unexpected results. In the case of a small rod-like body, elementary considerations based on the equation of motion suggest that in a steady flow  $\mathbf{n}$  aligns with the direction where  $\mathbf{A}$  has the greatest rate of strain. For our fully developed turbulent flow, we resolved the velocity gradient into its symmetric part  $\mathbf{S}$ , the rate of strain and its antisymmetric part  $\mathbf{\Omega}$ , the vorticity tensor, which corresponds to the vorticity vector  $\boldsymbol{\omega} = |\omega|\mathbf{e}_\omega$ . We determined the eigenvalues  $\lambda_i$  and normalized eigenvectors  $\mathbf{e}_i$  of  $\mathbf{S}$ , ordered so that  $\lambda_1 \geq \lambda_2 \geq \lambda_3$ . We examined the statistics of  $\mathbf{n} \cdot \mathbf{e}_i$  and  $\mathbf{n} \cdot \mathbf{e}_\omega$ , expecting to find that  $\mathbf{n}$  is most strongly aligned with  $\mathbf{e}_1$ . For rod-like particles in fully developed turbulent flow, however, we find that  $\mathbf{n}$  is much more strongly aligned with  $\mathbf{e}_\omega$ .

To gain insight into the alignment between the rod axis and the vorticity, we studied a simpler model obtained by replacing the velocity gradient matrix,  $\mathbf{A}(t)$ , by a fluctuating random matrix with prescribed statistics. In order to determine a suitable stochastic model, we also investigated the statistics of the velocity gradient matrix. Our results validate a model previously introduced by Vincenzi *et al* [12], in which the velocity gradients are obtained by independent Ornstein–Uhlenbeck processes [13, 14]. Specifically, elements of the strain rate and vorticity tensors are generated with different decay times,  $\tau_s$  and  $\tau_v$ , respectively [15]. Our results are generally consistent with those of earlier studies of velocity gradients [16–19].

Despite the fact that the stochastic model reproduces the statistics of the velocity gradient quite accurately, we find that when the synthetic velocity gradient  $\mathbf{A}(t)$  is inserted into the equation of motion for the axial vector  $\mathbf{n}(t)$ , the statistics are a very poor fit to the results obtained from simulations of turbulence. In particular, the stochastic model gives very weak alignment between  $\mathbf{n}$  and  $\mathbf{e}_\omega$ .

We discuss two possible mechanisms to explain the observed alignment between  $\mathbf{e}_\omega$  and  $\mathbf{n}$  in the limit of rod-like particles. One mechanism is present when  $\mathbf{A}(t)$  is generated by a stochastic process, and explains the weak alignment of  $\mathbf{n}$  and  $\mathbf{e}_\omega$  for the stochastic model. We also describe an alternative mechanism of alignment based on the relationship between the equations of motion of  $\mathbf{n}$  and  $\boldsymbol{\omega}$ . More specifically, in the absence of any viscous effect, the equation for the unit vector parallel to the vorticity is *exactly* the equation obtained by Jeffery for infinitely thin rods. Thus, the straining induced in the fluid tends to orient similarly vorticity and the direction of the rods. In this sense, the lack of perfect alignment between vorticity and the direction of the rods in direct numerical simulations (DNS) is merely a consequence of viscosity.

The alignment of very small rods in turbulent flows is also relevant to how material lines elongate, because the tangent to the material line obeys the same equation of motion as the rod axis. Elongation is induced by the stretching due to the turbulence, so the orientation of  $\mathbf{n}$  with respect to the strain eigenvectors determines how fast a line grows [20, 21]. It has been noted in particular in [20] that the rate of growth of material lines is significantly slower than expected if the lines were to align parallel to the strongest stretching direction. In this respect, the authors of [11] have noted some puzzling features, pointing to a very special alignment between the direction of the rods  $\mathbf{n}$  and the characteristic directions of the velocity gradient tensor,  $\mathbf{A}$ . The present work provides further insight into these issues.

Our paper is organized as follows. Section 2 discusses numerical results on the orientation of small bodies in fully developed turbulence. We report our results on the projection of  $\mathbf{n}$  onto the vectors  $\mathbf{e}_i$ ,  $\mathbf{e}_\omega$ . The correlation functions of the direction  $\mathbf{n}(t)$  of small rods are determined and compared with the corresponding correlation functions for small spheres. Section 3 discusses the correlation function of the velocity gradients and introduces a stochastic

model for  $\mathbf{A}(t)$ , equivalent to the model used in [12]. Section 3 also describes the results on the statistics of  $\mathbf{n}(t)$  for the case when we use the stochastic model for  $\mathbf{A}(t)$ . Section 4 considers two possible reasons for the alignment between rod-like particles and the vorticity vector. We argue that this alignment is a consequence of similarities between the equations of motion of  $\mathbf{n}$  and  $\boldsymbol{\omega}$ . Section 5 presents a brief conclusion.

## 2. Orientation statistics in turbulence

### 2.1. Equations of motion

We consider the motion of a microscopic ellipsoidal object in a turbulent velocity field  $\mathbf{u}(\mathbf{r}, t)$ . The object is assumed to be neutrally buoyant and smaller than the smallest lengthscale characterizing fluid motion, namely the Kolmogorov size,  $\eta_K \equiv (\nu^3/\mathcal{E})^{1/4}$ , where  $\mathcal{E}$  is the rate of turbulent energy dissipation per unit mass and  $\nu$  the viscosity of the fluid. The motion of the body is described by the position of its centre,  $\mathbf{r}(t)$ , and the direction of a unit vector aligned with its axis,  $\mathbf{n}(t)$ . In many applications the two ends of the body are indistinguishable, and the vector  $\mathbf{n}$  is non-oriented. It is also possible to do experiments where the two ends can be distinguished by a visible mark. The centre of the body is assumed to be advected by the fluid flow:  $\dot{\mathbf{r}} = \mathbf{u}(\mathbf{r}, t)$ .

The motion of microscopic bodies is determined by the velocity gradient matrix evaluated at the centre of the body, with elements

$$A_{ij}(t) = \frac{\partial u_i}{\partial r_j}(\mathbf{r}(t), t), \quad (1)$$

where  $\mathbf{r}(t)$  is the advected particle trajectory. We assume that the flow is incompressible, so that  $\sum_{i=1}^3 A_{ii} = 0$ . This tensor can be decomposed into a symmetric part  $\mathbf{S}$ , which is termed the strain rate, and an antisymmetric part  $\boldsymbol{\Omega}$ , which is the vorticity tensor:

$$\mathbf{A} = \mathbf{S} + \boldsymbol{\Omega}, \quad \mathbf{S}^T = \mathbf{S}, \quad \boldsymbol{\Omega}^T = -\boldsymbol{\Omega}. \quad (2)$$

The equation of motion of the director vector of a microscopic ellipsoidal body is [1]

$$\frac{d\mathbf{n}}{dt} = \boldsymbol{\Omega}(t)\mathbf{n} + \frac{\alpha^2 - 1}{\alpha^2 + 1}[\mathbf{S}(t)\mathbf{n} - (\mathbf{n} \cdot \mathbf{S}(t)\mathbf{n})\mathbf{n}], \quad (3)$$

where  $\alpha$  is the axis ratio of the ellipsoid. Bretherton [22] showed that the same equation of motion is applicable to any axisymmetric body, but in the general case there is no formula relating  $\alpha$  to the geometry of the body.

### 2.2. Numerical methods

The velocity field of the fluid,  $\mathbf{u}(\mathbf{r}, t)$ , was determined by solving directly the Navier–Stokes equation, in a triply periodic box, using pseudo-spectral methods [23]. The runs were carried out with  $N$  grid points in each of the three spatial directions and the resolution was varied in the range  $64 \leq N \leq 384$ , allowing us to cover a range of Reynolds numbers of  $45 \leq R_\lambda \leq 170$  with adequate numerical accuracy.

In addition, we determined numerically the motion of tracers in the flow. The velocity gradient tensor was followed along trajectories, and the equations for the deformation tensor  $\mathbf{W}$ , which determines the evolution of any passive vector advected and stretched by the flow, was

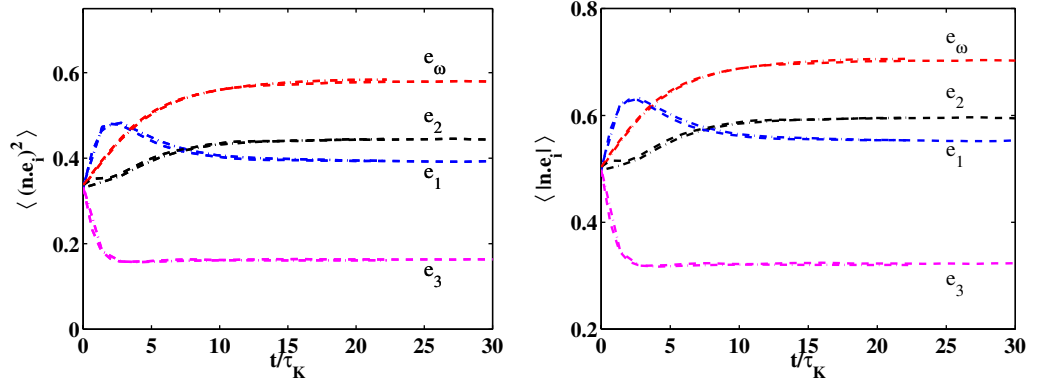


**Figure 1.** Alignment of rods in a turbulent flow: evolution alignment of  $\mathbf{n}$  with the eigenvalues of strain,  $\mathbf{e}_i$ , and the direction of vorticity,  $\mathbf{e}_\omega$ , with time. After a short transient, the mean values of  $|\mathbf{e}_i \cdot \mathbf{n}|$  and  $(\mathbf{e}_i \cdot \mathbf{n})^2$  reach a constant level, reflecting a tendency for  $\mathbf{n}$  to align with  $\mathbf{e}_2$  and  $\mathbf{e}_\omega$ , to be mostly perpendicular to  $\mathbf{e}_3$ , and no particular alignment with  $\mathbf{e}_1$ . The results obtained with Reynolds numbers  $R_\lambda = 83$  (dashed line) and  $R_\lambda = 170$  (dashed-dotted line) are superposed.

solved numerically [20, 23]. (The deformation tensor is also termed the *monodromy matrix*, and will be given the symbol  $\mathbf{M}$  when it is used later in this paper.) This provides us with a straightforward way to determine the evolution of a unit vector  $\mathbf{n}$ , and to obtain the solution of equation (3) by normalization [4, 5].

Statistics were accumulated by launching in the flow  $N_p$  particles and by following their orientation for a duration equal to at least  $\sim 20\tau_K$ . Averages over  $N_i$  time intervals were carried out, and the statistics shown here were obtained with  $N_i \times N_p$  greater than or equal to 250 000.

### 2.3. Single-time statistics

The real-symmetric matrix  $\mathbf{S}$  has three eigenvalues  $\lambda_i$ , ordered so that  $\lambda_1 \geq \lambda_2 \geq \lambda_3$ , and three orthonormal eigenvectors  $\mathbf{e}_i$ :

$$\mathbf{S}\mathbf{e}_i = \lambda_i\mathbf{e}_i. \quad (4)$$

The antisymmetric vorticity tensor with elements  $\Omega_{ij}$  corresponds to a vorticity vector  $\boldsymbol{\omega}$ , with magnitude  $\omega$  and unit direction vector  $\mathbf{e}_\omega$ :

$$\boldsymbol{\Omega} = \frac{1}{2} \begin{pmatrix} 0 & \omega_z & -\omega_y \\ -\omega_z & 0 & \omega_x \\ \omega_y & -\omega_x & 0 \end{pmatrix}, \quad \boldsymbol{\omega} = (\omega_x, \omega_y, \omega_z) = \omega\mathbf{e}_\omega. \quad (5)$$

We investigated the degree of overlap between  $\mathbf{n}$  and the vectors  $\mathbf{e}_i$  and  $\mathbf{e}_\omega$  for rod-like particles in fully developed turbulence. Figure 1 shows the evolution with time of  $\langle |\mathbf{n} \cdot \mathbf{e}_i| \rangle$  and  $\langle |\mathbf{n} \cdot \mathbf{e}_i|^2 \rangle$ . The rods were initiated with a fixed spatial direction:  $\mathbf{n}(t=0) = \mathbf{e}_x$ , i.e. with a random direction with respect to the directions associated with the velocity gradient tensor. At short times,  $0 \leq t/\tau_K \lesssim 3$ , the direction  $\mathbf{n}$  tends to align preferentially with the largest (stretching) eigendirection of the strain and to become perpendicular to the smallest (compressive) eigendirection of the strain. The quantities characterizing the statistical properties of alignment converged to constant

**Table 1.** Statistics characterizing the alignment of rod-like particles. The error bars on these numbers are not larger than 0.01. No significant difference has been observed when the Reynolds number varies in the range  $45 \leq R_\lambda \leq 170$ .

$\alpha \rightarrow \infty$ statistics	$\mathbf{n} \cdot \mathbf{e}_1$	$\mathbf{n} \cdot \mathbf{e}_2$	$\mathbf{n} \cdot \mathbf{e}_3$	$\mathbf{n} \cdot \mathbf{e}_\omega$
$\langle  X  \rangle$	0.55	0.59	0.32	0.70
$\langle X^2 \rangle$	0.39	0.44	0.17	0.58

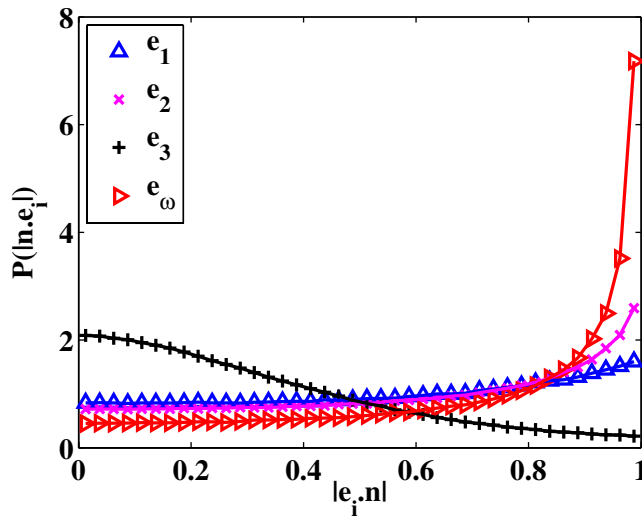


**Figure 2.** Alignment of rods in a turbulent flow: PDF of the cosine of the angle between  $\mathbf{n}$  and the eigenvectors of strain,  $\mathbf{e}_i$ , and the direction of vorticity,  $\mathbf{e}_\omega$ , in the steady-state regime. The PDFs reveal that  $\mathbf{n}$  tends to align with  $\mathbf{e}_\omega$ , to be perpendicular to  $\mathbf{e}_3$ , but do not show any particular alignment with  $\mathbf{e}_1$ . The Reynolds number of the flow is  $R_\lambda = 170$ .

values in a few multiples of the Kolmogorov time,  $\tau_K = \sqrt{\nu/\mathcal{E}}$ . The limiting values, listed in table 1, differ significantly from those of a random distribution of  $\mathbf{n}$ , which are  $\frac{1}{2}$  and  $\frac{1}{3}$ , respectively. The probability distribution functions (PDFs) of  $|\mathbf{n} \cdot \mathbf{e}_i|$  in the long-time asymptotic regime ( $t/\tau_K \gtrsim 20$ ) are plotted in figure 2. These data show an unexpected effect. From equation (3), it is expected that the direction vector will align with the principal axis of the rate of the strain tensor. Although there is some alignment with  $\mathbf{e}_1$ , there is a much stronger alignment between  $\mathbf{n}$  and  $\mathbf{e}_\omega$ , the direction of the vorticity vector. This unexpected result will be discussed in section 4. We also observe a correlation between  $\mathbf{n}$  and  $\mathbf{e}_2$ , which is consistent with the known alignment between  $\mathbf{e}_2$  and  $\mathbf{e}_\omega$  [24] and our observation of alignment between  $\mathbf{n}$  and  $\mathbf{e}_\omega$ .

By following directly the evolution of the two vectors  $\mathbf{n}$  and  $\mathbf{e}_\omega$  along Lagrangian trajectories, we observed events where the two vectors are essentially parallel over a relatively long duration, up to a few Kolmogorov times, separated by time intervals where the directions of the two vectors fluctuate with respect to each other.

In the limit of spherical particles (where  $\alpha = 0$ ), the axis  $\mathbf{n}$  is arbitrary, and these statistics take the values expected for a uniform distribution on the sphere, namely  $\langle |\mathbf{n} \cdot \mathbf{e}_i| \rangle = \frac{1}{2}$  and  $\langle |\mathbf{n} \cdot \mathbf{e}_i|^2 \rangle = \frac{1}{3}$ .

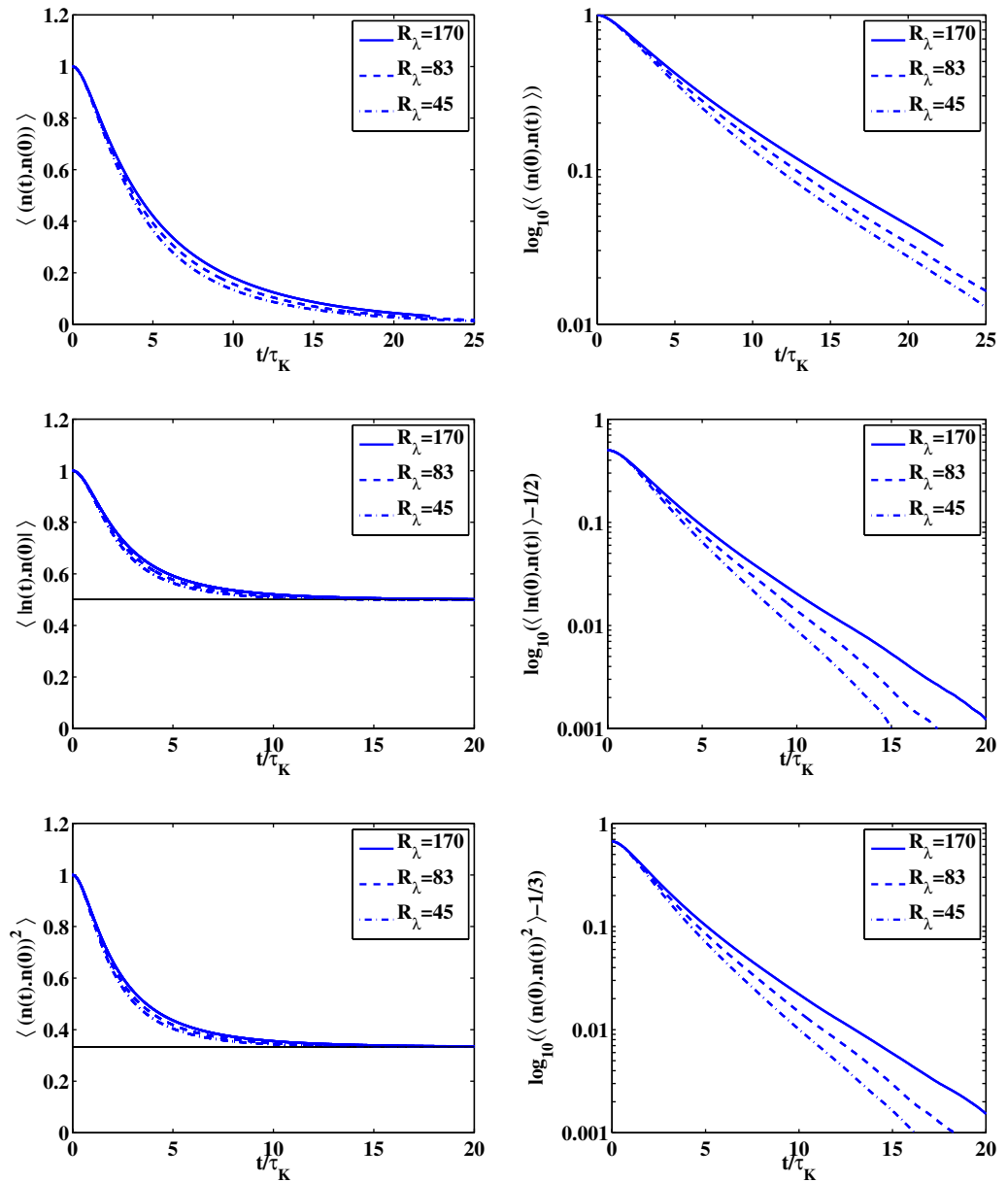


**Figure 3.** Correlation functions for rod-like particles: top:  $\langle \mathbf{n}(t) \cdot \mathbf{n}(0) \rangle$ ; middle:  $\langle |\mathbf{n}(t) \cdot \mathbf{n}(0)| \rangle$ ; bottom:  $\langle |\mathbf{n}(t) \cdot \mathbf{n}(0)|^2 \rangle$ . The correlation functions decay towards their asymptotic value for  $t \rightarrow \infty$  with a characteristic decay time,  $\tau$ . DNS results indicate that  $\tau/\tau_K \approx 2.6, 3.0$  and  $3.7$  for  $\langle |\mathbf{n}(t) \cdot \mathbf{n}(0)| \rangle$  and  $\langle (\mathbf{n}(t) \cdot \mathbf{n}(0))^2 \rangle$  at  $R_\lambda = 45, 83$  and  $170$ , respectively. For  $\langle (\mathbf{n}(t) \cdot \mathbf{n}(0)) \rangle$ , the decorrelation times are  $\tau/\tau_K \approx 6.1, 6.5$  and  $7.4$  at  $R_\lambda = 45, 83$  and  $170$ , respectively.

#### 2.4. Correlation functions

It is not yet possible to determine in a laboratory experiment the directions of the vectors  $\mathbf{e}_i$  at the same time as a particle is tracked. But the orientation of a particle could be determined by imaging techniques, and correlation functions of  $\mathbf{n}(t)$  could be evaluated. In figure 3, we

show the correlation functions  $\langle \mathbf{n}(t) \cdot \mathbf{n}(0) \rangle$ ,  $\langle |\mathbf{n}(t) \cdot \mathbf{n}(0)| \rangle$  and  $\langle |\mathbf{n}(t) \cdot \mathbf{n}(0)|^2 \rangle$ , respectively, for a rod-like particle. All these correlation functions start at  $\langle \mathbf{n}(0)^2 \rangle = 1$ , and decay towards their asymptotic limits, namely  $\lim_{t \rightarrow \infty} \langle \mathbf{n}(0) \cdot \mathbf{n}(t) \rangle = 0$ ,  $\lim_{t \rightarrow \infty} \langle (\mathbf{n}(0) \cdot \mathbf{n}(t))^2 \rangle = 1/3$  and  $\lim_{t \rightarrow \infty} \langle |\mathbf{n}(0) \cdot \mathbf{n}(t)| \rangle = 1/2$ , essentially exponentially; see the right column of figure 3. The decay rates of  $\langle (\mathbf{n}(0) \cdot \mathbf{n}(t))^2 \rangle$  and  $\langle |\mathbf{n}(0) \cdot \mathbf{n}(t)| \rangle$  are, at a given Reynolds number, very close to each other, but significantly different from the decay rate of  $\langle \mathbf{n}(0) \cdot \mathbf{n}(t) \rangle$ . For the latter correlation function, a much slower decay rate is observed. Expressed in terms of the Kolmogorov time, the decorrelation time slightly increases as a function of the Reynolds number; see figure 3.

Figure 4 shows the correlation functions of the orientation vector for an arbitrarily chosen axis through a spherical particle. As was the case for rod-like particles, the correlation function of orientation is observed to decay essentially exponentially when  $t \rightarrow \infty$ . The decay rate for spherical particles is higher than that for rod-like particles. As was the case for elongated particles, the characteristic decay time for spheres, when expressed in terms of the Kolmogorov time scale of the flow, increases with the Reynolds number. Also, the correlation functions  $\langle (\mathbf{n}(0) \cdot \mathbf{n}(t))^2 \rangle$  and  $\langle |\mathbf{n}(0) \cdot \mathbf{n}(t)| \rangle$  decay at very similar rates, at a given Reynolds number, whereas  $\langle \mathbf{n}(0) \cdot \mathbf{n}(t) \rangle$  decays much more slowly.

If the dynamics of  $\mathbf{n}(t)$  were described by diffusion on a spherical surface with angular diffusion coefficient  $D$ , these correlation functions would decay exponentially with rate constants corresponding to eigenvalues of the Laplacian operator on a sphere, namely  $\lambda_l = l(l+1)D$  with  $l = 0, 1, 2, \dots$ . The correlation function  $\langle \mathbf{n}(0) \cdot \mathbf{n}(t) \rangle$  would be determined by the  $l = 1$  mode, whereas the other correlations have a decay rate determined by the  $l = 2$  mode. This model therefore predicts that the ratio of decay rates is 3 : 1, which is not a good fit to the empirical data. In a separate work [26] we have defined and analysed a more complex model for random motion on a spherical surface, termed the spherical Ornstein–Uhlenbeck process. This model also does not provide a good fit for the correlation functions in figures 3 and 4.

### 3. Stochastic model for velocity gradients

#### 3.1. Lagrangian statistics of the velocity gradient

Because the evolution of  $\mathbf{n}(t)$  depends upon the velocity gradient matrix  $\mathbf{A}(t)$ , we also investigated the statistics of its elements  $A_{ij}(t)$ . We found that the correlation functions for fluctuations of matrix elements of the strain and vorticity are well approximated by exponential functions: for matrix elements of the vorticity, the correlation function is well approximated by

$$\langle \Omega_{ij}(t) \Omega_{ij}(0) \rangle = C_v \exp(-\gamma_v |t|). \quad (6)$$

The elements of the rate of the strain matrix have a similar correlation function, with the decay rate  $\gamma_v$  replaced by a different value of the rate constant,  $\gamma_s$ , and with a different prefactor. The decay rates of correlations of the diagonal and off-diagonal elements of the rate of strain are equal, but their prefactors are different, consistent with the values of the variances of the various components of strain in a homogeneous isotropic turbulent flow. The correlation functions of the diagonal elements of strain and of vorticity are shown in figure 5. The correlation function of the off-diagonal of strain, once divided by  $\langle S_{12}^2 \rangle$ , superposes with the correlation function of the diagonal component of strain. These results are consistent with earlier investigations. Girimaji and Pope [16] developed a complex model for velocity gradient statistics and found that the vorticity varies more slowly than the strain. Brunk *et al* [17] found that the spectral

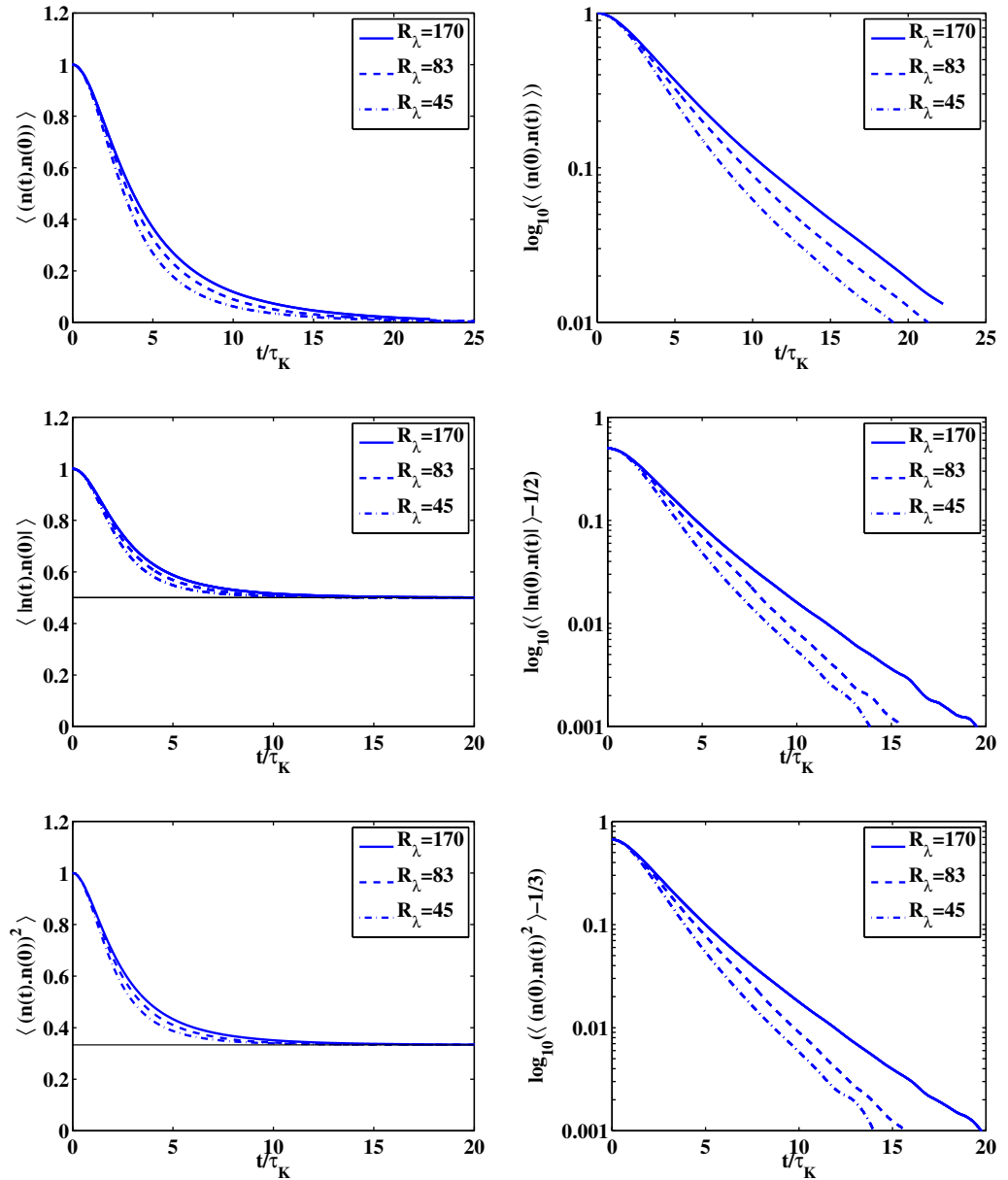


**Figure 4.** Correlation functions for spherical particles: top:  $\langle \mathbf{n}(t) \cdot \mathbf{n}(0) \rangle$ ; middle:  $\langle |\mathbf{n}(t) \cdot \mathbf{n}(0)| \rangle$ ; bottom:  $\langle |\mathbf{n}(t) \cdot \mathbf{n}(0)|^2 \rangle$ . The correlation functions decay towards their asymptotic value for  $t \rightarrow \infty$  with a characteristic decay time,  $\tau$ . DNS results indicate that  $\tau/\tau_K \approx 2.4, 2.6$  and  $3.3$  for  $\langle |\mathbf{n}(t) \cdot \mathbf{n}(0)| \rangle$  and  $\langle (\mathbf{n}(t) \cdot \mathbf{n}(0))^2 \rangle$  at  $R_\lambda = 45, 83$  and  $170$ , respectively. For  $\langle (\mathbf{n}(t) \cdot \mathbf{n}(0)) \rangle$ , the decorrelation times are  $\tau/\tau_K \approx 5.2, 5.35$  and  $5.6$  at  $R_\lambda = 45, 83$  and  $170$ , respectively.

intensity of fluctuations of the velocity gradient is well approximated by a Lorentzian function, which is consistent with our observation that the correlation function is well approximated by an exponential function. Our numerical data show little dependence of the decay rate of individual components of the strain and vorticity components on the Reynolds number:  $\gamma_v \approx (7.2\tau_K)^{-1}$  and  $\gamma_s \approx (2.3\tau_K)^{-1}$ , consistent with previous findings [12].

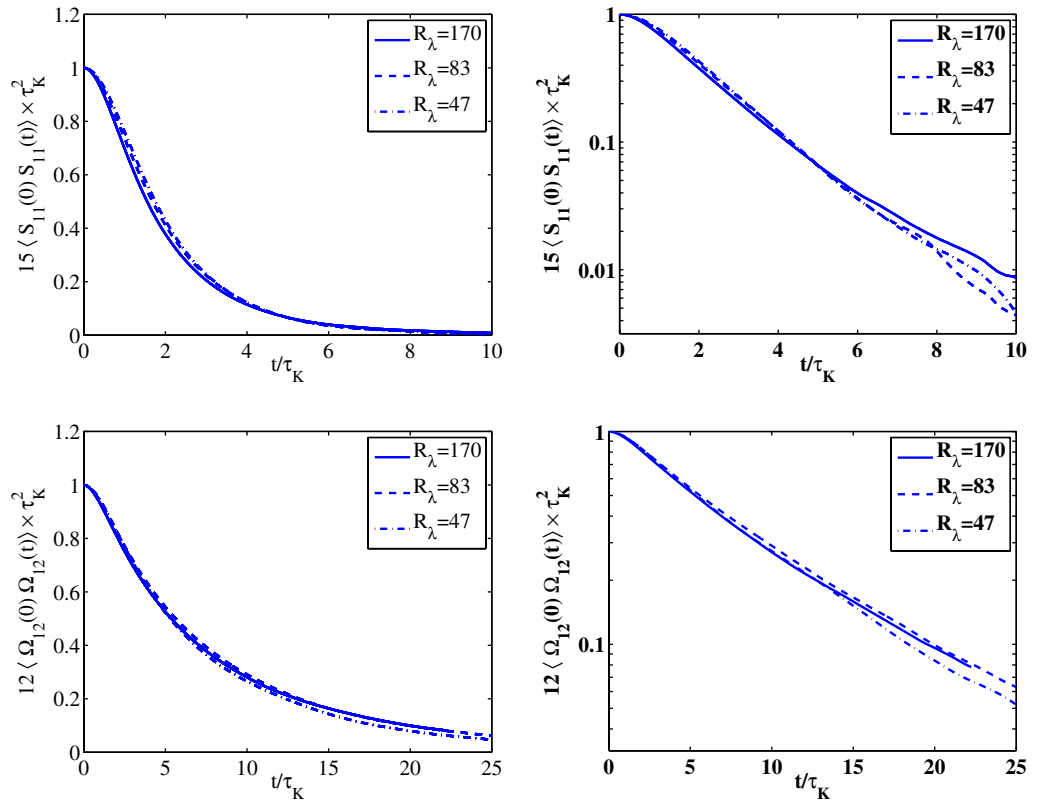


**Figure 5.** Correlation functions for elements of the velocity gradient matrix. Top: diagonal strain rate:  $\langle S_{ii}(t)S_{ii}(0) \rangle$ ; bottom: vorticity:  $\langle \Omega_{ij}(t)\Omega_{ij}(0) \rangle$ . Up to statistical fluctuations, the off-diagonal strain rate correlation function superposes the diagonal one.

Despite these relatively simple properties of the correlation between individual components of strain and vorticity, the decay of the norm of strain and vorticity has been demonstrated to show a strong Reynolds number dependence [15, 18, 19]. This is an indication that the simple Ornstein–Uhlenbeck approach used here to describe the evolution of the velocity gradient tensor in the flow misses some important aspects of the dynamics.

### 3.2. A model for the velocity gradient

In this section, we describe a simple stochastic model for the matrix  $\mathbf{A}(t)$ . The same model was used by Vincenzi *et al* [12], without giving full details; here we give a detailed account of its implementation. It is known that the elements of  $\mathbf{S}$  and  $\mathbf{\Omega}$  fluctuate randomly about zero, with different timescales  $\tau_s$  and  $\tau_v$ , respectively. Their correlation functions are well approximated by exponential functions. This suggests modelling the elements of  $\mathbf{S}$  and  $\mathbf{\Omega}$  by Ornstein–Uhlenbeck processes. The Ornstein–Uhlenbeck process [13, 14] is a stochastic differential equation for the time dependence of a variable  $x(t)$ :

$$\dot{x} = -\gamma x + \eta(t), \quad (7)$$

where  $\eta(t)$  is a white-noise signal satisfying

$$\langle \eta(t) \rangle = 0, \quad \langle \eta(t) \eta(t') \rangle = 2D\delta(t - t'). \quad (8)$$

We have argued that numerical evidence indicates that the vorticity components fluctuate on a different timescale than the strain-rate components, but that both have temporal correlation functions that are well described by exponential functions. This motivates the following approach to modelling the velocity gradients by a system of independent Ornstein–Uhlenbeck processes. The three independent components of the vorticity will be modelled by

$$\dot{\Omega}_{ij} = -\frac{1}{\tau_v} \Omega_{ij} + \sqrt{2D_v} \zeta_{ij}(t), \quad (9)$$

where  $\zeta_{ij}$  are elements of an antisymmetric matrix which are independent white-noise signals, with statistics  $\langle \zeta_{ij}(t) \rangle = 0$ ,  $\langle \zeta_{ij}(t) \zeta_{ij}(t') \rangle = \delta(t - t')$ . This model reproduces the exponential correlation function (6), with  $C_v = D_v \tau_v$  [13, 14]. The off-diagonal elements of the strain rate are modelled in the same way, but with a different relaxation time and diffusion coefficient,  $\tau_s$  and  $D_o$ .

$$\dot{S}_{ij} = -\frac{1}{\tau_s} S_{ij} + \sqrt{2D_o} \eta_{ij}(t), \quad (10)$$

where  $\eta_{ij}(t)$  are elements of a symmetric matrix which are independent white-noise signals. In both (9) and (10) we assume that  $i > j$ , and the coefficients with  $i < j$  are determined, respectively, by antisymmetry and by symmetry. The diagonal elements of the strain-rate matrix must satisfy  $\sum_{i=1}^3 E_{ii} = 0$ , which is the incompressibility condition,  $\nabla \cdot \mathbf{u} = 0$ . This constraint is satisfied by the solution of the following Ornstein–Uhlenbeck equations:

$$\dot{S}_{ii} = -\frac{1}{\tau_s} S_{ii} + \sqrt{2D_d} \left[ \eta_{ii}(t) - \frac{1}{3} \sum_{j=1}^3 \eta_{jj}(t) \right]. \quad (11)$$

The elements  $\Omega_{ij}$  and  $S_{ij}$  generated by these processes are statistically independent, apart from the constraint that  $\sum_i S_{ii} = 0$ . The variances of the off-diagonal, diagonal and vorticity elements are, respectively, denoted by  $\langle S_o^2 \rangle$ ,  $\langle S_d^2 \rangle$  and  $\langle \Omega^2 \rangle$ , and are related to the relaxation times and diffusion rates by

$$\langle S_o^2 \rangle = D_o \tau_s, \quad \langle S_d^2 \rangle = \frac{2}{3} D_d \tau_s, \quad \langle \Omega^2 \rangle = D_v \tau_v. \quad (12)$$

From the Navier–Stokes equation it is easy to see that  $\text{tr}(\mathbf{\Omega}^2) + \text{tr}(\mathbf{S}^2) = 0$  [25] and also that the rate of dissipation per unit mass is  $\mathcal{E} = \nu \text{tr}(\mathbf{A}^T \mathbf{A})$ . Together with the requirement that the statistics of the model are invariant under rotation, so that it describes the velocity gradient of isotropic turbulence, these relations can be used to determine the diffusion coefficients

$$D_d = 2D_o = \frac{1}{10\tau_K^2 \tau_s}, \quad D_v = \frac{1}{12\tau_K^2 \tau_v}, \quad (13)$$

where  $\tau_K = \sqrt{\nu/\mathcal{E}}$  is the Kolmogorov timescale of the turbulence.

### 3.3. Alignment statistics of the random matrix model

We examined the alignment of the axial vector  $\mathbf{n}(t)$  for rod-like particles, using the synthetic velocity gradient model for  $\mathbf{A}(t)$  described above, with the fitted decay times  $\tau_v$  and  $\tau_s$  (we used

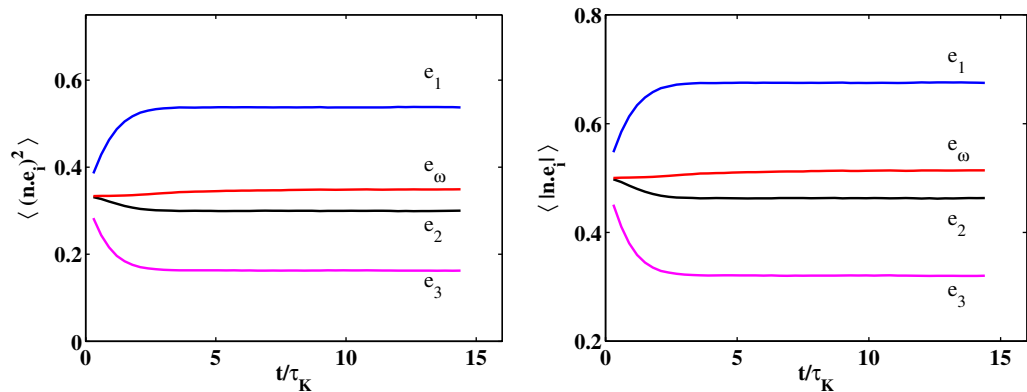


**Figure 6.** Solutions of the stochastic model: plots of the alignment of  $\mathbf{n}$  with the eigenvalues of strain,  $\mathbf{e}_i$ , and the direction of vorticity,  $\mathbf{e}_\omega$ , with time. After a short transient, the mean values of  $|\mathbf{e}_i \cdot \mathbf{n}|$  and  $(\mathbf{e}_i \cdot \mathbf{n})^2$  reach a constant level, reflecting a tendency for  $\mathbf{n}$  to align with  $\mathbf{e}_1$ , to be mostly perpendicular to  $\mathbf{e}_3$  and to show no particular trend of alignment with  $\mathbf{e}_2$  or  $\mathbf{e}_\omega$ .

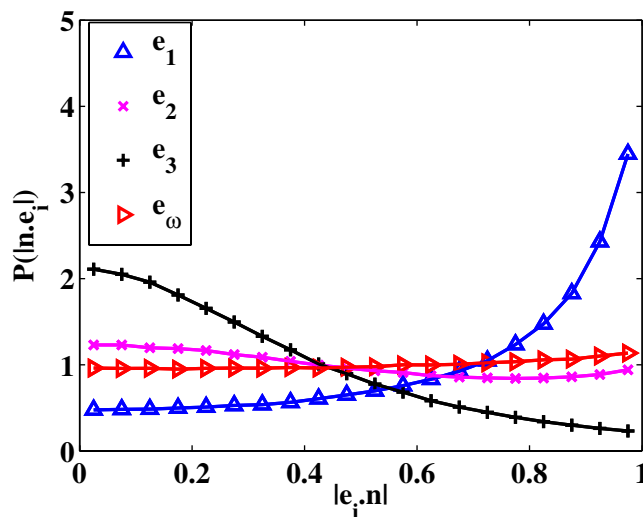


**Figure 7.** Solutions of the stochastic model: PDF of the cosine of the angle between  $\mathbf{n}$  and the eigenvectors of strain  $\mathbf{e}_i$  and the direction of vorticity  $\mathbf{e}_\omega$  in the steady-state regime. The PDFs reveal that  $\mathbf{n}$  tends to align with  $\mathbf{e}_1$ , to be perpendicular to  $\mathbf{e}_3$ , but does not show any particularly strong alignment with either  $\mathbf{e}_2$  or  $\mathbf{e}_\omega$ .

the values obtained from the simulation with the largest  $R_\lambda$ ). The results are shown in figure 6. They are markedly different from the dynamics of rod-like particles in true turbulence. The PDFs in the long-time limit are shown in figure 7. They are in agreement with the expectation that  $\mathbf{n}(t)$  will be preferentially aligned with  $\mathbf{e}_1$ . There is some degree of alignment between  $\mathbf{n}$  and  $\mathbf{e}_\omega$ , but this is a weak effect.

#### 4. Discussion of the alignment of rods with vorticity

A striking feature of the numerical data is that, in the case of rod-like particles, the axis  $\mathbf{n}$  shows a strong tendency to align with the vorticity vector  $\boldsymbol{\omega}$ . This effect was also present to a small degree when we replaced the true velocity gradient of Navier–Stokes turbulence with a stochastic model.

Here we consider two possible mechanisms that could explain this effect. First (in section 4.1) we examine the influence of the Navier–Stokes dynamics on the velocity gradient tensor  $\mathbf{A}$  and argue that this effect, which is not captured by the stochastic model, provides an explanation of the observed alignment between  $\mathbf{n}$  and vorticity. In section 4.2 we describe an alternative mechanism for alignment, which is present in the random strain model and which explains the weak alignment seen there.

##### 4.1. Relation between Jeffery’s equation and the vorticity equation

In the limit of rod-like particles, the equation of motion (3) for the direction vector becomes

$$\dot{\mathbf{n}} = \mathbf{A}\mathbf{n} - (\mathbf{n} \cdot \mathbf{A}\mathbf{n})\mathbf{n}. \quad (14)$$

The equation of motion for the vorticity vector can be expressed in the form

$$\frac{D\boldsymbol{\omega}}{Dt} = \mathbf{A}\boldsymbol{\omega} + \nu\nabla^2\boldsymbol{\omega}. \quad (15)$$

The term  $\mathbf{A}\boldsymbol{\omega}$  on the right-hand side of equation (15) is often written as  $\mathbf{A}\boldsymbol{\omega} = \mathbf{S}\boldsymbol{\omega}$ , in view of the identity  $\boldsymbol{\Omega}\boldsymbol{\omega} = 0$ . The term  $\mathbf{S}\boldsymbol{\omega}$  has the physical interpretation of vortex stretching, so the evolution of vorticity results from vortex stretching and viscous effects, represented by the two terms on the right-hand side of equation (15). Equation (14) can be solved by considering a companion linear equation [4]:

$$\dot{\mathbf{d}} = \mathbf{A}(t)\mathbf{d} \quad (16)$$

where  $\mathbf{d}(t)$  is initially equal to  $\mathbf{n}(0)$ . The solution of (14) is given by normalizing the vector  $\mathbf{d}(t)$ :

$$\mathbf{n}(t) = \frac{\mathbf{d}(t)}{|\mathbf{d}(t)|}. \quad (17)$$

The similarity of the equations of motion (15) and (16) indicates that the solution vectors  $\boldsymbol{\omega}$  and  $\mathbf{d}$  are expected to be correlated. We note that the vector  $\boldsymbol{\omega}$  remains bounded and has a stationary probability distribution, whereas the magnitude of  $\mathbf{d}$  is expected to increase exponentially at a rate determined by the Lyapunov exponent of the flow. It follows that the term  $\nu\nabla^2\boldsymbol{\omega}$  in (15) must be *comparable* in magnitude to  $\mathbf{A}\boldsymbol{\omega}$  in order for  $\boldsymbol{\omega}$  to remain finite. The equation of motion (15) therefore differs from (16) by the addition of a term that is of comparable magnitude. Correspondingly, we conclude that the correlation between the directions of  $\boldsymbol{\omega}$  and  $\mathbf{d}$  is neither very large nor very small. This argument is sufficient to explain the very significant, although not perfect correlation between the directions  $\mathbf{n}$  and  $\mathbf{e}_\omega$ . It would, however, be extremely challenging to make a quantitative theory out of this argument because of the difficulty of characterizing the statistics of  $\nabla^2\boldsymbol{\omega}$ .

A consequence of the arguments developed in the previous paragraph is that the vortex stretching term  $\mathbf{A}\boldsymbol{\omega}$  in equation (15) is responsible for the alignment of  $\mathbf{n}$  and  $\mathbf{e}_\omega$ , whereas the viscous term disrupts the alignment. While this argument cannot easily be quantified rigorously,

**Table 2.** Statistics characterizing the alignment of rod-like particles by a random matrix, following the Ornstein–Uhlenbeck model. The error bars on these numbers are not larger than 0.01.

$\alpha \rightarrow \infty$ statistics	$\mathbf{n} \cdot \mathbf{e}_1$	$\mathbf{n} \cdot \mathbf{e}_2$	$\mathbf{n} \cdot \mathbf{e}_3$	$\mathbf{n} \cdot \mathbf{e}_\omega$
$\langle  X  \rangle$	0.68	0.46	0.32	0.51
$\langle X^2 \rangle$	0.54	0.30	0.16	0.35

its consequences can be demonstrated numerically. For example, it is a simple matter to write the equation of evolution for the squared scalar product  $(\mathbf{n} \cdot \mathbf{e}_\omega)^2$  as a sum of a term coming from vortex stretching and of another term coming from viscosity in equation (15):

$$\frac{1}{2} \left\langle \frac{D(\mathbf{e}_\omega \cdot \mathbf{n})^2}{Dt} \right\rangle \equiv \frac{1}{2} \left\langle \frac{D(\mathbf{e}_\omega \cdot \mathbf{n})^2}{Dt} \right\rangle_{\text{str}} + \frac{1}{2} \left\langle \frac{D(\mathbf{e}_\omega \cdot \mathbf{n})^2}{Dt} \right\rangle_{\text{visc}}. \quad (18)$$

In the statistically steady state, the average of  $\langle ((\mathbf{n} \cdot \mathbf{e}_\omega)^2) \rangle$  is constant, so that both sides of (18) are equal to zero. The contribution due to the stretching term in the vorticity equation can be directly computed from DNS. Specifically, we find that

$$\begin{aligned} \frac{1}{2} \left\langle \frac{D(\mathbf{e}_\omega \cdot \mathbf{n})^2}{Dt} \right\rangle_{\text{str}} &= \langle (\mathbf{e}_\omega \cdot \mathbf{n})[(\mathbf{n} \cdot \mathbf{A}\mathbf{e}_\omega) + (\mathbf{e}_\omega \cdot \mathbf{A}\mathbf{n}) - (\mathbf{n} \cdot \mathbf{e}_\omega)[(\mathbf{e}_\omega \cdot \mathbf{A}\mathbf{e}_\omega) + (\mathbf{n} \cdot \mathbf{A}\mathbf{n})]] \rangle \\ &\approx 0.013\tau_K^{-1} > 0. \end{aligned} \quad (19)$$

In the limited range of Reynolds numbers simulated here ( $45 \lesssim R_\lambda \lesssim 170$ ) the rate of alignment indicated in equation (19) is positive, and its value is simply proportional to the inverse of the Kolmogorov time. This numerical observation demonstrates that in the steady state, the stretching term in the vorticity equation (15) tends to align the directions of  $\mathbf{n}$  and  $\mathbf{e}_\omega$ , consistent with the picture presented above.

#### 4.2. Alignment of direction in a random gradient field

A crucial strand of the argument presented in section 4.1 to explain the alignment between  $\mathbf{n}$  and  $\omega$  is the fact that both  $\mathbf{n}$  and  $\omega$  are influenced by the velocity gradient  $\mathbf{A}$ . In fact, from the Navier–Stokes equations, one deduces that  $\mathbf{A}$  obeys the following nonlinear equation of motion, in which the value of  $\mathbf{A}$  is itself influenced by the strain field:

$$\frac{D\mathbf{A}}{Dt} + \mathbf{A}^2 = -\frac{1}{\rho}\mathbf{H} + \nu\nabla^2\mathbf{A}, \quad (20)$$

where  $\mathbf{H}$  is the pressure Hessian, with elements  $H_{ij} = \partial^2 p / \partial x_i \partial x_j$ . In contrast, the model studied in section 3, where  $\mathbf{A}(t)$  is a random function of time that reproduces known statistical properties of the velocity gradient tensor, but that does not influence its own evolution, fails to produce the proper alignment. We note that a weak alignment between  $\mathbf{n}$  and  $\mathbf{e}_\omega$  was visible in the solution of the model; see table 2. Here we discuss how such an alignment can occur.

We have seen that the components of the rate of strain vary more rapidly than the vorticity. This feature suggests considering the equation of motion (14) in the case when the vorticity is slowly varying. It is convenient to solve equation (16) by introducing the matrix  $\mathbf{M}(t)$ , such that

for each value of  $j$ , the vector  $\mathbf{U}$  defined by  $U_i(t) \equiv M_{i,j}(t)$  is the solution of equation (16) with the initial condition  $U_i(0) = \delta_{ij}$ . Clearly, the matrix  $\mathbf{M}(t)$ , referred to here as the *monodromy matrix*, satisfies

$$\dot{\mathbf{M}} = \mathbf{A}(t)\mathbf{M}. \quad (21)$$

The solution of (16) is given by  $\mathbf{d}(t) = \mathbf{M}(t)\mathbf{n}(0)$ . It is instructive to isolate the effect of the vorticity in the equation of motion for the monodromy matrix,  $\mathbf{M}$ . We do this by introducing another monodromy matrix  $\mathbf{M}_0$  that evolves under the vorticity alone:

$$\dot{\mathbf{M}} = (\mathbf{S} + \boldsymbol{\Omega})\mathbf{M}, \quad \dot{\mathbf{M}}_0 = \boldsymbol{\Omega}\mathbf{M}_0. \quad (22)$$

The two monodromy matrices may be related by writing

$$\mathbf{M}(t) = \mathbf{M}_0(t)\mathbf{K}(t), \quad (23)$$

where  $\mathbf{K}(t)$  is an evolution matrix that describes the effect of the shear. An elementary calculation shows that  $\mathbf{K}$  has the equation of motion

$$\dot{\mathbf{K}} = \boldsymbol{\sigma}(t)\mathbf{K}, \quad (24)$$

where

$$\boldsymbol{\sigma} = \mathbf{M}_0^{-1}\mathbf{S}\mathbf{M}_0 \quad (25)$$

is a symmetric matrix, representing the effect of shear in a coordinate system that is rotated by the vorticity. Consider the form of the matrix  $\boldsymbol{\sigma}$  when the vorticity vector is frozen and equal to  $\boldsymbol{\Omega}_0$ . In this case the matrix  $\mathbf{M}_0$  is a rotation matrix:

$$\mathbf{M}_0 = \exp(\boldsymbol{\Omega}_0 t). \quad (26)$$

Without loss of generality we can consider the case when  $\boldsymbol{\omega}$  is aligned with the  $z$ -axis,  $\boldsymbol{\omega} = \omega\mathbf{e}_3$ , so that  $\mathbf{M}_0$  is a rotation matrix of the form

$$\mathbf{R}(\omega t) = \begin{pmatrix} \cos \omega t & -\sin \omega t & 0 \\ \sin \omega t & \cos \omega t & 0 \\ 0 & 0 & 1 \end{pmatrix} \equiv \begin{pmatrix} c & -s & 0 \\ s & c & 0 \\ 0 & 0 & 1 \end{pmatrix}. \quad (27)$$

If the elements of  $\mathbf{S}$  are  $S_{ij}$ , the elements of  $\boldsymbol{\sigma}$  are

$$\boldsymbol{\sigma} = \begin{pmatrix} c^2 S_{11} + s^2 S_{22} + 2cs S_{12} & (c^2 - s^2)S_{12} + cs(S_{22} - S_{11}) & cS_{13} - sS_{23} \\ (c^2 - s^2)S_{12} + cs(S_{22} - S_{11}) & s^2 S_{11} + c^2 S_{22} - 2cs S_{12} & cS_{23} + sS_{13} \\ cS_{13} - sS_{23} & cS_{23} + sS_{13} & S_{33} \end{pmatrix}. \quad (28)$$

Note that all of the off-diagonal components contain a factor that oscillates with angular frequency  $\omega$  or  $2\omega$ . If the frequency  $\omega$  exceeds the rate at which elements of  $\mathbf{S}(t)$  decorrelate, then the contribution of these off-diagonal elements to the evolution of the matrix  $\mathbf{K}$  will be suppressed. Furthermore, the non-oscillatory components of the first two diagonal elements, both of which are equal to  $\frac{1}{2}(S_{11} + S_{22}) = -\frac{1}{2}S_{33}$ , have a smaller variance than the third element,  $S_{33}$ . These considerations show that, when  $\omega$  is large compared to the decorrelation rate, the dominant action of the matrix  $\boldsymbol{\sigma}(t)$  in equation (24) is extension or compression along the  $\mathbf{e}_3$

axis. The inference that should be drawn from (28) is that when the vorticity is transformed out of the equation of motion to give (24), the effective strain-rate field  $\sigma$  is anisotropic, and may favour larger fluctuations of the components of  $\mathbf{n}$  along the axis of the vorticity vector  $\boldsymbol{\omega}$  than in the plane perpendicular to it. The analysis of models for anisotropic random strain will be the subject of a future publication.

## 5. Concluding remarks

Our numerical study of the evolution of rod-like particles in turbulent flows has allowed us to uncover important and surprising aspects concerning the orientation of the rods in relation to the directions characterizing the velocity gradient tensor,  $\mathbf{A}$ , of the flow.

Indications that the direction of the rods align in a peculiar way have been obtained by Shin and Koch [11], who noted that the rate of rotation measured in DNS cannot be simply deduced from the properties of the rate of strain tensor in the flow; in fact, the rate of rotation in turbulent flow is very significantly reduced, compared to what one may expect by assuming a purely isotropic distribution of  $\mathbf{n}$ . The results presented here characterize the alignment between the direction of the rods and those defined by the flow, and reveal strong alignment properties between the direction of the rods,  $\mathbf{n}$ , and the strain eigendirections and vorticity.

Two features of the alignment of rod-like particles in turbulent flows uncovered here were quite unexpected. Firstly, we have observed that the alignment statistics are very different if the velocity gradient matrix  $\mathbf{A}(t)$  derived from Navier–Stokes turbulence is replaced by a stochastic model, for which the correlation functions of the elements  $A_{ij}(t)$  are a good match to the turbulent data. This observation is in agreement with the results obtained by Shin and Koch [11] for finite-sized rods, as well as with the observed property that the growth of line elements proceeds slowly, compared to simple predictions based on the fastest stretching rate [20]. As we argue in this work, the difference between the simple stochastic model and the actual solutions of the Navier–Stokes equations is due to the essential property that the evolution of the vorticity is influenced in a crucial way by the velocity gradient tensor  $\mathbf{A}$ .

The second surprising result is that in turbulent flows the direction  $\mathbf{n}$  of rod-like particles is correlated with the vorticity  $\boldsymbol{\omega}$  much more strongly than with the principal strain axis  $\mathbf{e}_1$ . In section 4, we have discussed two possible mechanisms that could lead to the observed correlation between the direction of vorticity and that of the rods. One mechanism, discussed in section 4.2, relies upon the strain field being anisotropic when expressed in a coordinate frame that rotates under the action of the vorticity. This effect is present in the random velocity gradient model considered in section 3.2, but it was found to be weak. The other mechanism, which was discussed in section 4.1 and which proved to be more significant, rests on a more detailed understanding of the dynamics of the rods and of the vorticity. Namely, the evolution equations for both  $\mathbf{n}$  and  $\boldsymbol{\omega}$  involve similar straining effects, the main difference between the two being due to viscosity, which acts only on vorticity. By separating the straining and the viscous terms in the vorticity equations, we have explicitly demonstrated that the alignment effect is induced by the straining term.

A further observation on the failure of stochastic models was made recently in the case of rotations of spherical particles in turbulence, which might be expected to be accurately described by a spherical Ornstein–Uhlenbeck model describing the random motion of a unit vector on a spherical surface [26]. This model is equivalent to Jeffery’s equation of motion in the limit of spherical particles, and the correlation function of vorticity is also an exponential function in

the spherical Ornstein–Uhlenbeck model. Somewhat surprisingly, we find that the correlation function of the axial vector of spherical particles in turbulence is markedly different from that of the spherical Ornstein–Uhlenbeck process.

## Acknowledgments

MW thanks the ENS Lyon for a visiting position. AP was supported by the Agence Nationale pour la Recherche under the contract DSPET, by IDRIS for computer resources and by the COST action MP0806. Both authors benefited from the hospitality of the Kavli Institute for Theoretical Physics in Santa Barbara, which is supported in part by the US National Science Foundation under grant number PHY05-51164.

## References

- [1] Jeffery G B 1922 The motion of ellipsoidal particles immersed in a viscous fluid *Proc. R. Soc. A* **102** 16
- [2] Lipscomb G G, Denn M M, Hur D U and Boger D V 1988 The flow of fiber suspensions in complex geometries *J. Non-Newtonian Fluid Mech.* **26** 297
- [3] Feng J J, Sgalari G and Leal L G 2000 A theory for flowing nematic polymers with orientational distortion *J. Rheol.* **44** 1085
- [4] Szeri A J 1993 Pattern formation in recirculating flows of suspensions of orientable particles *Phil. Trans. R. Soc. A* **345** 477
- [5] Wilkinson M, Mehlig B and Bezuglyy V 2009 Fingerprints of random flows *Phys. Fluids* **21** 043304
- [6] Bezuglyy V, Mehlig B and Wilkinson M 2010 Poincare indices of rheoscopic visualisations *Europhys. Lett.* **89** 34003
- [7] Wilkinson M, Bezuglyy V and Mehlig B 2011 Emergent order in rheoscopic swirls *J. Fluid Mech.* **667** 158–87
- [8] Zimmermann R, Gasteuil Y, Bourgoin M, Volk R, Pumir A and Pinton J F 2011 Rotational intermittency and turbulence induced lift experienced by large particles in a turbulent flow *Phys. Rev. Lett.* **106** 154501
- [9] Zimmermann R, Gasteuil Y, Bourgoin M, Volk R, Pumir A and Pinton J F 2011 Tracking the dynamics of translation and absolute orientation of a sphere in a turbulent flow *Rev. Sci. Instrum.* **82** 0333906
- [10] Parsa S, Guasto J S, Kishore M, Ouellette N T, Gollub J P and Voth G A 2011 Rotation and alignment of rods in two-dimensional chaotic flow *Phys. Fluids* **23** 043302
- [11] Shin M and Koch D L 2005 Rotational and translational dispersion of fibres in isotropic turbulent flows *J. Fluid Mech.* **540** 143
- [12] Vincenzi D, Jin S, Bodenschatz E and Collins L R 2007 Stretching of polymers in isotropic turbulence: a statistical closure *Phys. Rev. Lett.* **98** 024503
- [13] Uhlenbeck G E and Ornstein L S 1930 On the theory of the Brownian motion *Phys. Rev.* **36** 823–41
- [14] van Kampen N G 1981 *Stochastic Processes in Physics and Chemistry* 2nd edn (Amsterdam: North-Holland)
- [15] Yeung P K, Pope S B, Kurth E A and Lamorgese A G 2007 Lagrangian conditional statistics, acceleration and local relative motion in numerically simulated isotropic turbulence *J. Fluid Mech.* **582** 399
- [16] Girimaji S S and Pope S B 1990 A diffusion model for velocity gradients in turbulence *Phys. Fluids A* **2** 242–56
- [17] Brunk B K, Koch D L and Lion L W 1998 Turbulent coagulation of colloidal particles *J. Fluid Mech.* **364** 81–113
- [18] Yu H and Meneveau C 2009 Lagrangian refined Kolmogorov similarity hypothesis for gradient time evolution and correlation in turbulent flows *Phys. Rev. Lett.* **104** 084502
- [19] Benzi R, Biferale L, Calzavarini E, Lohse D and Toschi F 2009 Velocity gradient statistics along particle trajectories in turbulent flows: the refined similarity hypothesis in the Lagrangian frame *Phys. Rev. E* **80** 066318

- [20] Girimaji S S and Pope S B 1990 Material-element deformation in isotropic turbulence *J. Fluid Mech.* **220** 427–568
- [21] Guala M, Lüthi B, Liberzon A, Tsinober A and Kinzelbach W 2005 On the evolution of material lines and vorticity in homogeneous turbulence *J. Fluid Mech.* **533** 339–59
- [22] Bretherton F P 1962 The motion of rigid particles in a shear flow at low Reynolds number *J. Fluid Mech.* **14** 284–304
- [23] Falkovich G and Pumir A 2007 Sling effect in collision of water droplets in turbulent clouds *J. Atmos. Sci.* **64** 4497–505
- [24] Ashurst W T, Kerstein A R, Kerr R M and Gibson C H 1987 Alignment of vorticity and scalar gradient with strain rate in simulated Navier–Stokes turbulence *Phys. Fluids* **30** 2343
- [25] Betchov R 1956 An inequality concerning the production of vorticity in isotropic turbulence *J. Fluid Mech.* **1** 497–504
- [26] Wilkinson M and Pumir A 2011 Spherical Ornstein–Uhlenbeck processes *J. Stat. Phys.* to appear (doi:10.1007/s-10955-011-0332-6) (arXiv:1105:4903)